

## Structure-Property Relationships of Smectic Liquid Crystalline Polyacrylates as Revealed by SAXS

Fabiano V. Pereira,<sup>\*,a</sup> Redouane Borsali,<sup>b</sup> Olga M.S. Ritter,<sup>a</sup> Paulo F. Gonçalves,<sup>a</sup>  
Aloir A. Merlo<sup>a</sup> and Nadya P. da Silveira<sup>a</sup>

<sup>a</sup>Instituto de Química, Universidade Federal do Rio Grande do Sul, Av. Bento Gonçalves, 9500,  
91501-970 Porto Alegre-RS, Brazil

<sup>b</sup>LCPO CNRS-ENSCP, Bordeaux 1 University, 16 Avenue Pey Berland 33607 Pessac, France

A influência da estrutura química dos grupos mesogênicos e do tamanho dos grupos espaçadores, no comportamento de fase de uma série de cristais líquidos poliméricos de cadeia lateral (SCLCP), foram estudados utilizando-se espalhamento de raios-X a Baixo Ângulo (SAXS) e Microscopia Ótica de Luz Polarizada (POM). Análises do arranjo das mesofases em amostras não orientadas e orientadas por ação do campo magnético são descritas. O papel do tamanho do espaçador lateral no empacotamento local e na largura da camada esmética determinados nas mesofases SmA e SmC é elucidado. Os ângulos  $\theta$  formados entre os grupos mesogênicos e a normal às camadas nas mesofases SmC foram determinados. Um estudo a respeito do grau de ordem em função da temperatura, para os polímeros esméticos foi possível através de medidas de SAXS. Uma ordenação particular em um dos SCLCPs estudados é relacionada com a coexistência de duas fases distintas.

The influence of the chemical structure of the mesogenic groups and the length of the spacer groups on the phase behavior in a series of side-chain liquid crystalline polyacrylates (SCLCP) have been studied using Small Angle X-ray Scattering (SAXS) and Polarized Optical Microscopy (POM). Analyses of the mesophase arrangement in unaligned and aligned samples by magnetic field are reported. The role of the spacer length on the local packing and on the thickness of the layers encountered in the SmA and SmC mesophases is elucidated. The tilt angles  $\theta$  of the mesogenic cores related to the normal of the layers in the SmC mesophases are measured. A study about the degree of order as a function of temperature for the smectic polymers was possible using SAXS measurements. A particular arrangement in one of the studied SCLCPs is related to the coexistence of two different phases.

**Keywords:** polyacrylates, SAXS, smectic phase, mesophase behavior, liquid-crystalline polymers

### Introduction

The research in basic liquid crystalline science and technological applications of liquid crystal (LCs) materials have experienced great growth due to their application in the design of optical and electro-optic devices.<sup>1</sup> Polymers containing mesogenic side groups attached laterally in a main chain are known as side chain liquid crystalline polymers (SCLCP) because of their liquid crystalline bulk properties.<sup>2</sup> Moreover, chirality in smectic (Sm) liquid crystals gained a pivotal position in the history of LCs after the discovery of the ferroelectricity in chiral SmC

molecules by Meyer and coworkers.<sup>3,4</sup> However, the first chiral SCLCP was reported in 1984 by Shibaev and *et al.*<sup>5</sup> Since then, a wide range of candidate materials has been synthesized and their mesomorphic and electro-optical properties have been studied as well.<sup>6-9</sup>

Together with the interest in the liquid crystal area, we have synthesized and studied the correlation structure-property in a series of different thermotropic liquid crystalline polyacrylates. In a previous paper we have reported the synthesis and mesomorphic behavior of two achiral liquid crystalline polyacrylates containing both 4'-*n*-alkoxyphenyl 4-[1-(propenyloxy)butyloxy]benzoate as mesogenic lateral groups.<sup>10</sup> Two different polymers having a short spacer with

\* e-mail: fabiano@iq.urfgs.br

four methylene units but different terminal tails in the lateral mesogenic groups have been studied. In another paper<sup>11</sup> we have described the synthesis, mesomorphic properties and solution behavior of new chiral polyacrylates derived from (*S*)-2-methyl-1-butanol as chiral terminal chain with spacer groups having either four or eleven carbon atoms. The polyacrylate with four methylene units in the spacer exhibits a chiral nematic phase, whereas the polyacrylate having a spacer containing eleven methylene units displays a smectic phase. More recently<sup>9</sup> we have reported the synthesis and mesomorphic properties of a chiral SCLCP containing (2*S*, 3*S*)-4-[1-(2-chloro-3-methyl)pentyl]oxy]phenyl 4-[1-(propenoyloxy)alkyloxy]benzoates, being the chiral terminal chain derived from L-isoleucine.

In the present contribution some aspects of the structure-property relationship and mesophase behavior are discussed referring to different SCLCPs reported elsewhere.<sup>9-11</sup> We selected four compounds having chiral and achiral mesogenic side groups with similar theoretical size but different number of carbons in the spacers and the terminal tail. X-ray scattering was used in order to, firstly allow unequivocal mesophase characterization of the polymers and, secondly, elucidate the local packing of the mesogenic units and the polymer backbones by comparing the experimental X-ray results with those obtained from molecular models. The orientation effect of the lateral mesogenic groups and the backbone using a magnetic field have also been examined to a full characterization of the liquid crystalline polymer mesophase.

## Experimental

The SCLCPs were synthesized using direct radical polymerization of a mesogenic methacrylate monomer. Details of the synthesis are described elsewhere.<sup>9-11</sup> General chemical structures of the liquid crystal polyacrylates are given in Figure 1.

While the polyacrylates  $P_{48}$  and  $P_{410}$  have small spacers containing only 4 methylene carbons, the  $P_{11M}$  and  $P_{11Cl}$  polymers have more flexible spacers with 11 carbon atoms. On the other hand,  $P_{11M}$  and  $P_{11Cl}$  present small terminal tails, whereas  $P_{48}$  and  $P_{410}$  have, respectively, 8 and 10 alkyl carbons as terminal tails. In this way, for all the samples, the mesogens comprising the spacers and terminal tails have the same lengths as we could verify through theoretical calculations. Similar polymers to  $P_{11M}$  and  $P_{11Cl}$ , having four carbons as spacers, instead of eleven, present only a nematic phase. These nematic polymers were the subject of other papers<sup>9,11</sup> and are not the aim of this work.

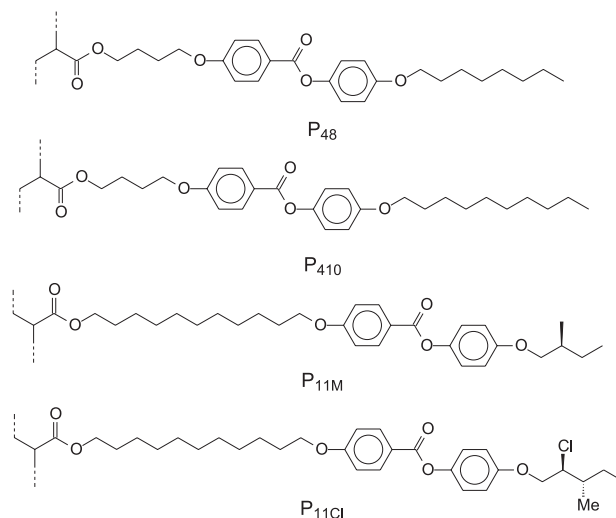


**Figure 1.** General chemical structure of the new liquid crystal polyacrylates.

X-ray measurements for the unaligned samples have been made with the powder samples placed in capillaries with 1 mm of diameter.

Single domains in liquid crystalline polymers can be obtained using an external field or mechanical orientation. A possible way to achieve the latter is fiber drawing. However, it is often an ill-defined process which can lead to controversial results. The use of fibers can also be untrustworthy because two different kinds of organization may be trapped in the skin and in the core of the fiber which results in complicated X-ray scattering patterns.<sup>12</sup> In this work the samples have been oriented through the application of a magnetic field, because it is the most convenient and conventional method to relate the scattered pattern of this kind of sample to their molecular arrangement.

The SAXS patterns of aligned samples were collected using some previously aligned once by a magnetic field. For this orientation, successive processes of heating and cooling near the smectic-isotropic transition temperature of the polymers have been made over a period of 24 h in a 12 T magnetic field. We were able to heat the samples up to 120 °C in the presence of the magnetic field. Afterwards, the samples have been cooled at approximately 0.3 °C min<sup>-1</sup> from isotropic phase to room temperature in the same magnetic field. The alignment in  $P_{410}$  and  $P_{48}$  polymers was not possible to carry out because their smectic - isotropic (Sm-Iso) temperature transitions (155 °C for  $P_{48}$  and 142 °C for  $P_{410}$ ) could not be achieved in the setup used for the orientation.

The SAXS measurements were carried out using a computer-controlled Nanostar X-ray system. The X-rays were generated from a rotating anode producing CuK $\alpha$  radiation ( $\lambda=1.54$  Å) in a vacuum chamber. A collimated

beam was passed horizontally through an evacuated chamber containing the sample and diffracted on a 2-D area detector. The sample was suspended vertically, at an adequate distance from the detector, in a hot stage and the temperature was controlled up to 200 °C with an accuracy of  $\pm 0.1$  °C. Both unaligned and aligned samples have been studied using this setup.

The measurements were made from room temperature up to the isotropic phase for all samples. An exposure time ranging from 1 to 4 hours was required. The image treatment has made taking the 360° into account.

Some results were obtained on the bending magnetic beamline BM2 at the European Synchrotron Radiation Facility (ESRF), Grenoble, France. In the ESRF  $\lambda$  was 0.775 Å and an indirect illumination CCD detector (Princeton Instruments) was used at 55.0 cm from the sample. Only the unaligned samples have been studied using this setup and the exposure times were about 50 s in this case. Silver behenate was used for calibration purposes in both equipments.

Theoretical calculations were used to estimate the length of the full mesogenic units for all the polymers in this work (and it was called  $l$ ). The geometries of the molecules were fully optimized using the MOPAC93r2<sup>13</sup> package at MNDO/PM3<sup>14</sup> semi empirical level. These optimized geometries were used as input to the GEPOL93<sup>15</sup> package, locally modified to calculate the molecular length in the longitudinal molecular axis. Afterwards, the Van der Waals radii of the atoms, as found in Paling's set,<sup>16</sup> in the two extremities of the covalent structure were added to the length of the longitudinal axis.

Optical textures were observed using a polarizing microscope Olympus BX41 equipped with a programmable Quasar MT300 heating stage. The samples were placed between glass slides, without any previous treatment. A PL-DSC and a Perkin-Elmer apparatus were used to identify thermal transitions operating at a scanning rate of 10 °C min<sup>-1</sup>. The molecular data and phase transitions of the studied polyacrylates are compiled in Table 1.

**Table 1.** Molecular weights,  $M_n$  (g mol<sup>-1</sup>), molecular weight distribution,  $M_w/M_n$  and thermal properties (T/°C) of the polyacrylates. g = glassy state, SmC = smectic C mesophase, SmA = smectic A mesophase, I = isotropic liquid

Polymer	$M_n$	$M_w/M_n$	g	SmC	SmA	I
P <sub>48</sub>	12700	1.54	. 58	. 130	. 155	.
P <sub>410</sub>	10400	1.61	. 57	. 108	. 142	.
P <sub>11M</sub>	25800	3.33	. 61	-	. 110	.
P <sub>11Cl</sub>	21200	1.63	. 37	-	. 68	.

$M_n$  and  $M_w/M_n$  were determined using size exclusion chromatography (SEC); transition temperatures were determined using DSC measurements, except for SmC-SmA transition, determined from POM.

## Results and Discussion

### Unaligned samples

It is well known that for a characterization of a tilted phase, like SmC, a homeotropic alignment can be helpful. It gives the possibility of analyzing the small biaxiality (when the phase has two optic axes) found in this mesophase.<sup>2</sup> In the case of a homeotropic alignment of the SmA phase the polarized light is unaffected by the material and so light can not pass through the analyzer. Another way, in the SmC phase it is not optically extinct. However, in general the phase characterization can be well done in non-treated surfaces offering advantages for the mesophase identification because both types of alignment (homeotropic and homogeneous) can occur at different positions of the microscope slide. In this way, the POM measurements in this work have been carried out using non-treated glass slides.

Figure 2 shows optical micrographs obtained on cooling for P<sub>48</sub>, P<sub>410</sub> and P<sub>11Cl</sub> polyacrylates. Figure 2a and 2b present, respectively, SmC (75 °C) and SmA (120 °C) textures for P<sub>410</sub> obtained on cooling. Figure 2c shows the SmC texture obtained in P<sub>48</sub> polymer (59 °C) whereas Figure 2d presents a SmA fan-texture obtained from P<sub>11Cl</sub> sample at 55 °C. The SmC textures present the fan-shaped texture broken, with the appearance of equidistant lines on the surface of the fan, characteristic for this mesophase.<sup>2</sup> P<sub>11M</sub> sample showed the same focal-conic SmA textures presented here for P<sub>11Cl</sub>.

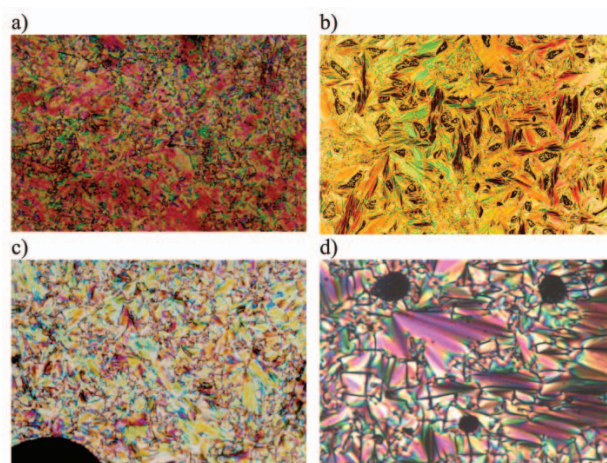


**Figure 2.** Optical micrographs (60x) of the SmC (a) and SmA (b) mesophases of the P<sub>410</sub> at 75 °C and 120 °C, respectively. SmC optical texture of the P<sub>48</sub> at 59 °C (c) and a fan-texture (SmA) of the P<sub>11Cl</sub> at 55 °C (d).

The X-ray scattering patterns for all studied unaligned samples in the smectic phases present the reflections consisting of circles with nearly uniform intensities. It

indicates that smectic layers were formed with no preferred direction in the samples without previous treatment.

The scattering patterns typically exhibit at least two rings with Bragg spacing in the 1:2 ratio in the  $q$ -range of  $\approx 0.08 - 0.4 \text{ \AA}^{-1}$  and a diffuse ring in the wide-angle region ( $q \approx 1.1 \text{ \AA}^{-1}$ ). The smectic layer length  $d$  is obtained from the position of the first inner ring by means of the Bragg relation  $d=2\pi/q$ .<sup>17</sup>

Figures 3 and 4 show the temperature dependence of the small angle X-ray scattering profiles for all the studied polyacrylates in a large temperature range. Figure 3 shows the scattering profiles from the polymers containing a small number of alkyl carbons as spacer,  $P_{48}$  and  $P_{410}$ , whereas Figure 4 shows the scattering profiles from the  $P_{11M}$  and  $P_{11Cl}$ , which have 11 methylene units as spacer. The X-ray intensities obtained from the  $P_{11Cl}$  sample are considerably weaker due to the chlorine atom localized at the mesogenic lateral group.

For  $P_{48}$  and  $P_{410}$ , both Bragg scattering peaks are sharp (Figure 3), indicating a pronounced confinement of the backbone layers between the mesogenic groups. However, the reflection localized at  $q \approx 0.4 \text{ \AA}^{-1}$  for

$P_{11M}$  and  $P_{11Cl}$  are diffuse (Figure 4). In fact, these diffuse scattering peaks are not attributed to the second-order Bragg reflections. It can also be observed in the isotropic phase of the polymer and may be attributed to the underlying polymer backbone.<sup>9</sup> Longer spacers as in  $P_{11M}$  and  $P_{11Cl}$  are more flexible and allow the main chain to reach a higher entropy and in this circumstances, some chains can occupy the space between the layers producing a diffuse scattered signal in the X-ray profile.<sup>18,19</sup>

Measurements performed at the beamline BM2 at the ESRF with these polymers in the mesophase showed the presence of a sharp second-order Bragg peak at the same position of the diffuse signals for  $P_{11M}$  and  $P_{11Cl}$ . In fact, it can also be seen in the X-ray scattering profiles of the  $P_{11M}$  obtained from the NANOSTAR X-ray source. The second-order Bragg peak is more clearly identified in the curves at 80 and 110 °C, in Figure 4a.

In a SmA mesophase the molecular long axes of the mesogenic groups is perpendicular with respect to the layer normal whereas in a SmC this axes is tilted with respect to the plane of the smectic layers.

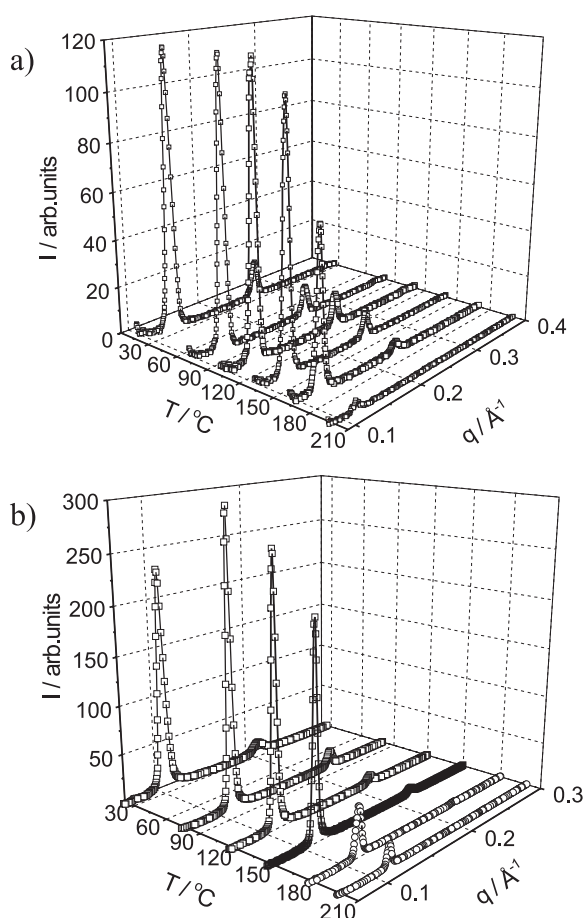


Figure 3. Temperature dependence of  $P_{48}$  (a) and  $P_{410}$  (b).

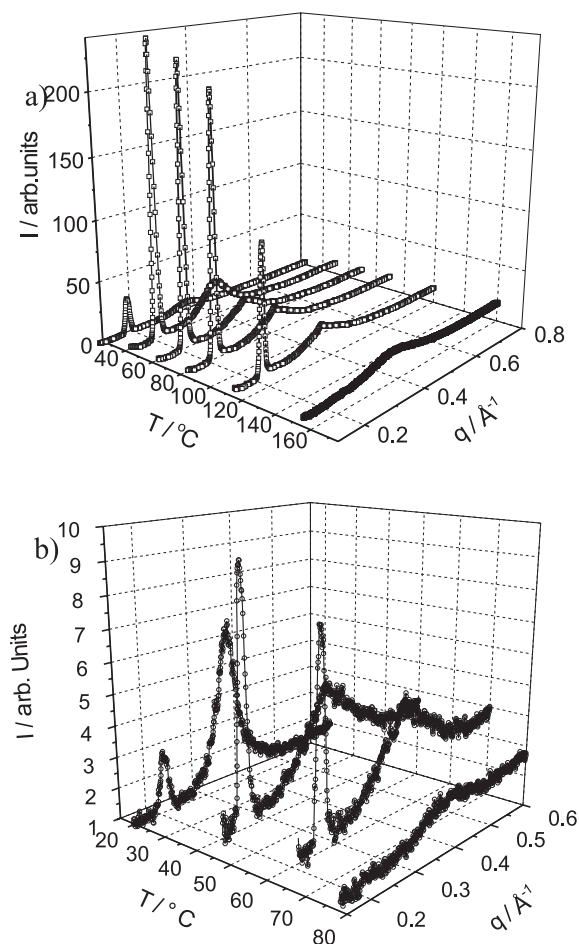
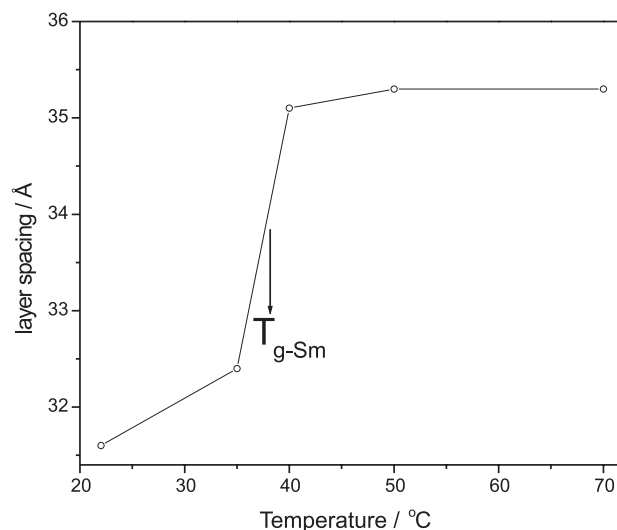


Figure 4. Temperature dependence of  $P_{11M}$  (a) and  $P_{11Cl}$  (b).

In the SmA and SmC mesophases, typically the SAXS profiles present two peaks having wave vector  $q = 2\pi/d$  for the first order reflection and  $q = 4\pi/d$  for the second order. Small changes in the layer thickness observed from the peak positions in the SAXS profiles for the studied polymers could be associated to two possibilities: amplitude motion of the mesogenic units attached to the polymer backbone due to the temperature<sup>9</sup> or, in the case of  $P_{48}$  and  $P_{410}$  homopolymers, due to the tilt of the mesogenic lateral groups to the normal of the layers (SmC mesophase). Unfortunately, we were not able to measure the tilted angle directly from the scattering patterns obtained by X-ray measurements because of the high Sm-Iso temperature transition that made the align process difficult to be applied in the isotropic phase of the sample. However, typical SmC textures from POM (Figure 2) were obtained for both  $P_{48}$  and  $P_{410}$  samples and the observed transition temperatures obtained by this technique are presented in Table 1. Moreover, the smectic layer thickness obtained using SAXS measurements increase at the same temperature range observed by optical microscopy for SmC-SmA transition, on heating. These values change from 49 to 53 Å for  $P_{48}$  and from 55 to 58 Å for  $P_{410}$ . If we consider that in a SmA mesophase the mesogenic groups are perpendicular to the main chain, the tilt angle in the SmC mesophase can be evaluated using the relation  $\theta = \cos^{-1}(d_{SmC} / d_{SmA})$ . In this relation  $d_{SmC}$  is the layer thickness in the SmC mesophase whereas  $d_{SmA}$  is the layer thickness in the SmA mesophase. For a given sample, we have considered that the interdigitation degree between the mesogens in the SmC is the same evaluated to the SmA mesophase. Using that, we calculated the imposed tilt angle of the mesogenic groups to the normal of the layer for the SmC mesophases as being 22.4° for  $P_{48}$  and 18.5° for  $P_{410}$  polymer.

A particular behavior was observed for  $P_{11Cl}$  polyacrylate, as can be seen in Figure 5. The inner peak for this sample corresponds to a layer of 31.1 Å in the glassy state (25 °C) and 35.3 Å in the mesophase (between 39 and 70 °C). The full mesogen length of the side chain estimated using theoretical calculations for this polymer is 36.94 Å.

The result showed in Figure 5 is an indication that besides the high degree of interdigitation between the lateral mesogens (100%), there is another effect that makes the layer length considerably lesser in the glass phase than the calculated value. It could be related to a conformational change of the mesogenic group in the glassy-smectic transition. The stereochemistry of the mesogenic group from single crystal X-ray structure determination<sup>9</sup> indicates that the tail group (where is found the chloro atom) is perpendicular to the mesogen in the solid state.



**Figure 5.** Temperature dependence of the smectic layer length of the  $P_{11Cl}$  polyacrylate.

In this way, the conformational changes in the mesogenic lateral group in the g-Sm temperature transition may be responsible for the change in the layer length. Interesting enough, this phenomenon has not been detected in the  $P_{11M}$  polymer, emphasizing the role of the chloro atom in the  $P_{11Cl}$  conformation.

Using semi-empirical calculations combined to SAXS results we can explain the local packing for the smectic layers of the studied homopolymers. The layer thickness ( $d$ ) and the proposed local packing for  $P_{410}$  and  $P_{11M}$  in the temperatures where these polymers present SmA mesophases are given in Figure 6.

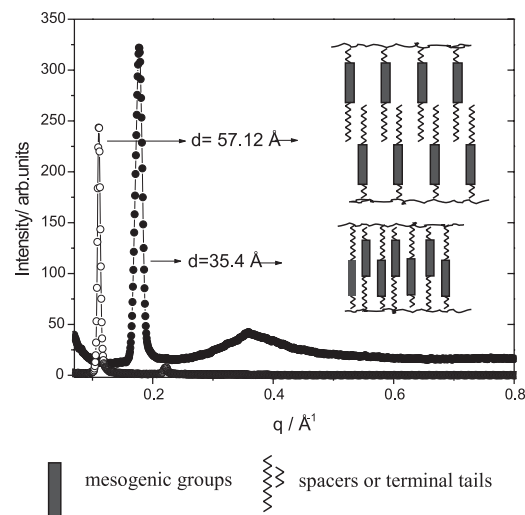


**Figure 6.** Small angle X-ray scattering profiles of the polyacrylates  $P_{410}$  at 140 °C (o) and  $P_{11M}$  at 70 °C (•).

Although these polyacrylates present the same length of the mesogenic groups, a great difference in the measured layer thickness can be observed. From these

**Table 2.** Measured layer spacing,  $d$  in the  $\text{Sm}_A$  mesophases, theoretical lengths of the mesogenic groups with spacers,  $l$ , the  $d/l$  relation and lateral spacing for two mesogenic groups,  $d_2$

	$d$	$l$	$d/l$	$d_2$
$P_{48}$	52.8	31.92	1.65	5.50
$P_{410}$	57.12	34.20	1.67	5.26
$P_{11M}$	35.4	36.94	0.96	5.48
$P_{11Cl}$	35.3	36.94	0.96	5.27

$d_2$ ,  $d$  and  $l$  values are given in angstroms;  $d$  and  $d_2$  were obtained at temperatures in the smectic phase;  $l$  was determined by semi-empirical geometric optimisation.

results, the local packing in each case can be elucidated. The different behavior in the overlapping degree and the consequent distance between the layers from different chains are due to the different flexibility of the alkyl spacers and the terminal tail.

Theoretical values of the full mesogen length,  $l$  together with the lengths  $d$  determined from SAXS are given in Table 2. The values of  $d$  are given for the temperatures where the polymers are in the smectic phases. For  $P_{48}$  and  $P_{410}$  the  $d/l$  relation in the  $\text{Sm}_A$  phase was determined to be 1.65 and 1.67, respectively. From these results we concluded that there is not a great interdigitation between the mesogenic groups from dissimilar chains. The value  $d/l > 1$  (for  $P_{48}$  and  $P_{410}$ ) can be related to a  $\text{Sm}_A$  phase.<sup>20</sup> If the liquid-crystalline polymer contains a short spacer as in  $P_{48}$  and  $P_{410}$ , there is not enough flexibility of the mesogenic moieties between the layers to allow a great interdigitation, imposing a limit in the approach between chains. Comparing these polymers, the  $d/l$  values are very close. It indicates a very similar local packing for  $P_{48}$  and  $P_{410}$ , imposed by the rigidity of the spacers that avoids a greater interdigitation. We can conclude that the mesogenic groups for these polymers present around 35% of interdigitation degree.

If the spacer is long enough, as in  $P_{11M}$  and  $P_{11Cl}$ , there is a great overlap of the lateral groups due to the flexibility of the spacers. At temperatures where  $P_{11Cl}$  is smectic, the layer thickness is similar to the size of the full mesogen obtained from theoretical calculations (Table 2). In this way, for  $P_{11M}$  and  $P_{11Cl}$ , where  $d/l = 0.96$  we can conclude a great overlap of the mesogenic units (near to 100% of interdigitation) from different chains. This relation is associated to a  $\text{Sm}_A$  mesophase.<sup>20</sup> In this kind of arrangement, a layer structure with a periodicity  $d$  slightly less than the molecular length  $l$  can be explained due to a combination of imperfect molecular orientational order and conformational disorder in the molecules.<sup>20</sup>

Both  $\text{Sm}_A$  and  $\text{Sm}_A$  arrangements of the chains are represented in the inset in Figure 6. The  $\text{Sm}_A$  arrangement is represented for the polymer having  $d=57.12 \text{ \AA}$  ( $P_{410}$ )

and the  $\text{Sm}_A$  is proposed for the polymer having  $d=35.4 \text{ \AA}$  ( $P_{11M}$ ). The local packing for  $P_{48}$  is similar to  $P_{410}$  and the chain arrangements in  $P_{11Cl}$  are similar to  $P_{11M}$ . It is assumed here that the change in the  $\text{Sm}_C$  layer thickness for  $P_{48}$  and  $P_{410}$  is only due to the tilt of the lateral mesogenic groups.

The maintenance of the smectic peaks in the Figures 3 and 4 at temperatures considered as isotropic for the polymers may be due to the existence of small regions of smectic materials, which could not be detected by means of DSC ( $\text{Sm}$ -Iso temperature transitions, given in Table 1). At the same way, the order associated to the underlying polymer backbone of  $P_{11M}$  and  $P_{11Cl}$  (which has a lesser degree of order if compared to the smectic peaks) could not be detected by means of DSC measurements.

In the wide angle region, the diffuse scattering ring is associated to the intermolecular interference in the direction perpendicular to the director and corresponds to the lateral spacing between two mesogenic groups attached to the polymer backbone. In this work this distance is namely  $d_2$  ( $q \approx 1.1 \text{ \AA}^{-1}$  for all samples studied). Since the lateral arrangement of the mesogenic groups are the same in the studied samples, the measured values of  $d_2$  are similar for all the studied liquid crystalline polymers. All  $d_2$  values vary between 5.2 and 5.5  $\text{\AA}$  and are given in Table 2 where the results obtained by analysis of the SAXS profiles are summarized.

It is known that the intensity of the low angle smectic layer maximum depends on the form factor  $F$  of the chain plus mesogenic units<sup>21</sup> and on the order parameter  $\tau_1$ ,  $I \propto (\tau_1 F)^2$ . If we assume that the form factor is constant, the order parameter is proportional to  $I^{1/2}$  and we can study their temperature dependence by measuring the intensity. Figure 7 shows the temperature dependence of the normalized intensity,  $I/I_{\text{max}}$ , of the first order layer reflections for the studied polyacrylates. The temperature

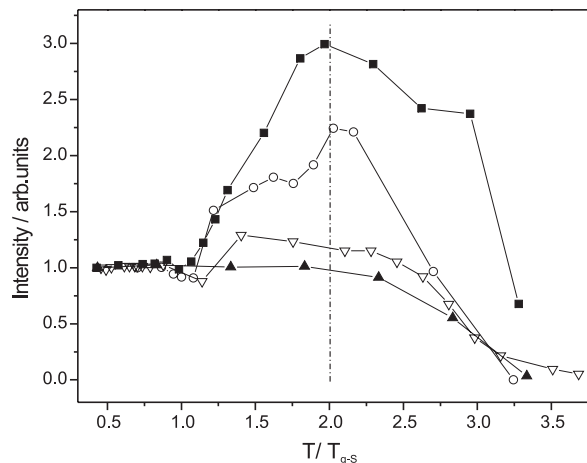


**Figure 7.** Temperature dependence of the intensity of the layer reflections in  $P_{11M}$  (■),  $P_{11Cl}$  (○),  $P_{410}$  (▽) and  $P_{48}$  (▲).

is shown as  $T/T_{g-Sm}$ , where  $T_{g-Sm}$  is the transition temperature from the glassy state to the smectic phase for each sample. The intensity first increases with the temperature and reaches a maximum in the smectic phase, about two times the  $T_{g-Sm}$  value. The intensity increase as a function of the temperature suggests a higher degree of smectic order. The increasing mobility of the main chain makes a higher intermolecular interaction between the mesogenic groups possible.<sup>22</sup> This phenomenon results in a higher confinement of the chains and the smectic layers becomes more defined.

This effect is stronger for the SCLCPs with more flexible spacers ( $P_{11M}$  and  $P_{11Cl}$ ), which present the second diffuse scattering peak. As discussed previously, the second-order Bragg peak appears in the temperatures where these polymers are smectic. Additionally the intensity of the first-order Bragg peak increases, indicating a higher degree of order by temperature increase. For  $P_{48}$  and  $P_{410}$  polymers, this effect is not pronounced because in these polymers the smectic layers are sufficiently defined in the entire temperature range studied. In  $P_{48}$  there is no increase of the intensity when  $T < 2.0 T_{g-Sm}$  and in  $P_{410}$  only a slightly effect is observed, with an intensity almost constant up to  $T \cong 2.0 T_{g-Sm}$ . The confinement of the backbone layers between the mesogens in these polymers have been discussed previously and can be seen comparing Figures 3 and 4.

The highest degree of order for all studied polymers was found at  $\cong 2.0 T_{g-Sm}$ . From these results we can conclude that the polymeric chains are more confined in the smectic layers for the temperature values near  $2.0 T_{g-Sm}$ . When the temperature increases beyond  $2.0 T_{g-Sm}$ , there is a decrease of the intensity, indicating that the motions of the backbone and the lateral groups begin to destroy the smectic ordering and reduces the number of regions with ordered structures inside the sample.

#### Aligned samples

The use of aligned (monodomain) samples is essential for detailed structural studies of liquid crystals<sup>20</sup> and are indicated for two main reasons: the information about relative angles between structural features is often lost by powder averaging and the signal-to-noise ratio is improved.<sup>23</sup> In this work, the aligned domains were obtained applying a magnetic field as explained in the experimental section.

In the aligned samples, the reflections have regions of higher intensity - the spots - indicating that smectic layers have a preferred direction. It can be seen in Figure 8 where the diffraction pattern for a)  $P_{11M}$  at 70 °C, b)  $P_{11Cl}$  at 40 °C

and c)  $P_{11Cl}$  at 55 °C are shown. Unfortunately, the  $P_{48}$  polymer was not susceptible to this treatment and the  $P_{410}$  presented only a weak orientation due to the high Sm-Iso temperature transition for both polymers. Figures 8a and 8b were obtained from a SAXS experiment and the pattern showed in Figure 8c was obtained in a simultaneous Wide and Small Angle X-ray Scattering experiment. The magnetic field direction ( $\vec{H}$ ) is indicated in each scattering pattern.

While the reflections in 7a and b are from polymeric chains, the scattering patterns in 7c present the reflections from the main chain (reflections from the small angle) and from the lateral mesogenic groups (wide angle). The reflections from the smectic layers are in a perpendicular direction to the  $\vec{H}$  because the magnetic field aligns the lateral groups. It can be clearly observed in the simultaneous SAXS/WAXS experiment (c), where the Bragg reflections from the mesogenic groups (wide angles) are parallel to the magnetic field direction and perpendicular to the reflections from the smectic layers (small angles).

All the SAXS patterns in Figure 8 are characteristic for a SmA phase. Furthermore, no changes in the smectic

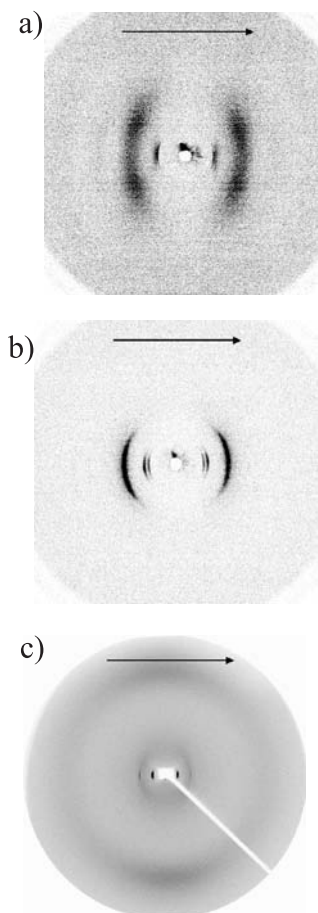


**Figure 8.** Small angle X-ray scattering patterns of the aligned polyacrylates: a)  $P_{11M}$  at 70 °C, b)  $P_{11Cl}$  at 40 °C and c) simultaneous SAXS and WAXS pattern of the aligned  $P_{11Cl}$  at 55 °C. The magnetic field direction is indicated in each SAXS pattern.

arrangement for the samples due to the aligning process were detected. The same arrangement and interdigitation degree of the lateral groups were found in aligned and unaligned samples.

The SAXS pattern obtained from the oriented samples shows that the diffuse diffraction signal located at  $q=0.4 \text{ \AA}^{-1}$  is oriented in the same direction of the polymer main chain (Figures 8a and 8b). This result provides a support for the statement that the origin of this signal is attributed to the underlying polymer backbone.

As far as the temperature dependence of the intensity is concerned, the behavior in the aligned samples is very similar to the one described for the unaligned.

A particular behavior could be seen for the oriented  $P_{11Cl}$  from 35 to 50 °C. Firstly, for the unaligned  $P_{11Cl}$  sample, the transition temperature from the glassy to the smectic state is characterized by a dislocation of the first Bragg reflection. With the orientation promoted by the magnetic field, the patterns showed in 8b are characteristic for the aligned sample between 35 and 50 °C. A third peak begins to appear at 35 °C and the SAXS pattern presents two inner peaks near to each other at 40 °C (Figure 8b), corresponding to the coexistence of a smectic and a glassy phase. The SAXS patterns obtained for this polymer were similar up to 50 °C. Additionally, the reflection at wide angles (in Figure 8c, at the same direction of the magnetic field) becomes sharper if compared to the reflection when the polymer is unaligned. When the sample is unaligned, this reflection is quite diffuse because the mesogenic lateral groups do not have a preferential orientation. The application of the magnetic field in the polymer orients the mesogenic groups and the reflections become sharper. The reflections at small angles become sharper also because the orientation of the lateral groups confine the main chain.

Moreover, the magnetic field produced a coexistence of phases (glassy and smectic) in the sample due to the constraint imposed by the magnetic field that makes difficult the  $T_{g-Sm}$  transition. In fact, instead of the well-defined temperature transition ( $T_{g-Sm}=37 \text{ °C}$ ) found in the unaligned sample, a large temperature range (35-50 °C) is observed when the sample is oriented. As a consequence, in this temperature range the system presents some regions in the glassy state and others in the smectic phase originating the two inner rings observed in Figure 8b. From 50 °C to the isotropic temperature the smectic layers present the same thickness of the non-oriented sample.

Another sample with the same structure of  $P_{11Cl}$  but with  $M_w = 9700$  presented the same behavior, showing that it is a characteristic related to the chemical structure of the mesogenic group of the polyacrylate.

## Conclusions

The structure-property relationships have been studied in four smectic side chain liquid-crystalline polymers containing the same mesogenic core and similar full mesogen lengths. The polymers having more flexible spacers ( $P_{11M}$  and  $P_{11Cl}$ ) presented only SmA mesophase whereas the polymers with rigid spacers ( $P_{48}$  and  $P_{410}$ ) showed SmA and SmC mesophase.

The layer smectic thickness, the local packing of the ribbons and, consequently, the interdigitation degree between the lateral mesogens is defined by the spacer length and has been fully characterized using X-ray experiments. The important role of the spacers is evidenced comparing the layer thickness between the polymers presenting four and eleven carbons as spacers. Having four carbons as spacers,  $P_{48}$  and  $P_{410}$  showed a  $SmA_d$  mesophase with 35% of lateral groups interdigitation due to the rigidity of the spacers that impose a limit in the approach between chains. If the spacer is long enough (eleven carbons as spacers as in the case of  $P_{11M}$  and in  $P_{11Cl}$ ) there is a great overlap of the lateral groups due to the flexibility of the spacers. In that case, a  $SmA_1$  mesophase appeared meaning about 100% of interdigitation degree of the mesogenic groups. The SmC tilt angle was determined as being 22.4° for  $P_{48}$  and 18.5° for  $P_{410}$ .

Interestingly, the highest smectic order was found at temperatures corresponding to  $2.0 T_{g-Sm}$ , meaning that a higher intermolecular interaction between the mesogenic groups is reached in this temperature.

The constraint imposed by the magnetic field in the aligned  $P_{11Cl}$  produced a coexistence of a glassy and smectic A phase.

## Acknowledgments

This work was supported by the Brazilian Secretary for Science and Technology by the program PADCT. F.V.P. acknowledges a P.H.D. fellowship from CNPq/Brazil. We are grateful to Dr. Marie-France Achard for helpful and discussions.

## References

1. Blackwood, K. M.; *Science* **1996**, *273*, 909.
2. Collings, P.J.; Hird, M.; *Introduction to Liquid Crystals Chemistry and Physics*, Taylor & Francis: London, 1997.
3. Meyer, R.B.; Liébert, L.; Strzelecki, L.; Keller, P.; *J. Phys.* **1975**, *36*, L69.
4. Meyer, R.B.; *Mol. Cryst. Liquid Cryst.* **1977**, *40*, 33.
5. Shibaev, V.P.; Kozlovsky, M.; Beresnev, L.; Blinov, L.; Platé, N.; *Polym. Bull.* **1984**, *12*, 299.

6. Busson, P.; Ihre, H.; Örtengren, J.; Gedde, U.W.; Hult, A.; Anderson, G.; *Macromolecules* **2001**, *34*, 1221.
7. Baxter, B.C.; Gin, D.L.; *Macromolecules* **1998**, *31*, 4419.
8. Robinson, W.K.; Carboni, C.; Kloess, P.; Perkins, S. P.; Coles, H.J.; *Liq. Cryst.* **1998**, *25*, 301.
9. Ritter, O.M.S; Merlo, A. A; Pereira, F.V.; da Silveira, N.P; Geissler, E.; Schpector, J.Z.; *Liq. Cryst.* **2002**, *29*, 1187.
10. Merlo, A. A.; Magnago, R.V.; Vollmer, A.F.; Mauller, R.S.; Pereira, F.V.; da Silveira, N.P.; *Polym. Bull.* **1999**, *42*, 551.
11. Merlo, A. A.; Ritter, O.M.; Pereira, F.V.; da Silveira, N.P.; *J. Braz. Chem. Soc.* **2001**, *12*, 184.
12. Mingos, D.M.P.; *Liquid Crystals II*, Springer-Verlag: Berlin Heidelberg, 1999.
13. Stewart, J. J. P.; Mopac 93.00 Manual revision number 2, Fujitsu Limited: Tokyo, 1993.
14. Stewart, J. J. P.; *J. Comput. Chem.* **1989**, *10*, 209.
15. Silla, E.; Tun, I.; Pascual-Ahuir, J.L.; *J. Comput. Chem.* **1991**, *9*, 1077.
16. Weast, R.C; *Handbook of Chemistry and Physics*, CRC Press: Cleveland, 1981.
17. Ebbut, J.; Richardson, R. M., Blackmore, J.; Mc Donnell, D.G.; *Mol. Cryst. Liquid Cryst.* **1995**, *261*, 549.
18. Noirez, L.; Boeffel, C.; Daouad-Aladine, A.; *Phys. Rev. Lett.* **1998**, *80*, 1453.
19. Davidson, P; *Liquid Crystals II*, Springer Verlag: Berlin, 1999.
20. D.Demus, J.; Goodby, G.W.; Gray, H.-W.; Spiess, V. Vill; *Handbook of Liquid Crystals*, Wiley-VCH: Weinheim, 1997.
21. Richardson, R. M.; Herring, N. J.; *Mol. Cryst. Liquid Cryst.* **1985**, *123*, 143.
22. Shuterlang, H.H.; Rawas, A.; *Mol. Cryst. Liquid Cryst.* **1986**, *138*, 179.
23. Davidson P.; *Prog. Polym. Sci.* **1996**, *21*, 893.

Received: August, 23, 2005

Published on the web: February 13, 2006